한국지반공학회논문집 제22권 4호 2006년 4월 pp. 61 ~ 71

Numerical Modeling of Sloping Ground under Earthquake Loading Using UBCSAND Model

UBCSAND모델을 이용한 사면의 동적거동해석

Park, Sung-Sik[1] 박 성 식
Kim, Young-Su[2] 김 영 수
Kim, Hee-Joong[3] 김 희 중

요 지

본 논문에서는 유효응력모델을 이용하여 포화된 사면의 동적거동에 관한 연구를 수행하였다. 수치해석에는 저자가 개발한 연성 유효응력모델인 UBCSAND모델을 이용하였으며, 이 모델은 초기전단응력이 수평면에 작용하는 경우와 작용하지 않는 경우를 포함한 반복 직접단순전단시험 자료를 이용하여 검증하였다. 검증된 모델은 느슨한 Fraser River 모래로 성형된 사면을 가진 원심모형모델의 동적거동을 예측하였다. 예측된 과잉간극수압, 가속도 및 변위를 계측치와 서로 비교하였으며, 예측치와 계측치는 비교적 서로 잘 일치하였다. 전단응력도의 응력전환형태는 초기전단응력과 반복전단응력의 크기에 따라 달라지며, 이는 지진시 포화된 사면의 안정해석에 아주 중요한 역할을 하고 있음을 알 수 있었다. 전단응력도의 응력전환이 발생하지 않을 경우에 사면근처의 모래는 낮은 유효응력 구속압과 그에 따른 팽창성으로(부의 과잉간극수압발생) 유효응력이 증가하여, 동적하중 하의 사면의 변위를 저지하였다. 이와 같은 유효응력모델은 액상화를 고려한 지반구조물의 내진해석에 유용하게 사용될 수 있다.

Abstract

A numerical procedure is presented for evaluating seismic liquefaction on sloping ground sites. The procedure uses a fully coupled dynamic effective stress analysis with a plastic constitutive model called UBCSAND. The model was first calibrated against laboratory element behavior. This involved cyclic simple shear tests performed on loose sand with and without initial static shear stress. The numerical procedure is then verified by predicting a centrifuge test with a slope performed on loose Fraser River sand. The predicted excess pore pressures, accelerations and displacements are compared with the measurements. The results are shown to be in good agreement. The shear stress reversal patterns depend on static and cyclic shear stress levels and are shown to play a key role in evaluating liquefaction response in sloping ground sites. The sand near the slope has low effective confining stress and dilates more. When no stress reversals occur, the sand behaves in a stiffer manner that curtails the accumulated downslope displacements. The numerical procedure using UBCSAND can serve as a guide for design of new soil structures or retrofit of existing ones.

Keywords : Centrifuge test, Liquefaction, Slope, Simple shear, Stress reversal, UBCSAND

1 정회원, Klohn Crippen Berger Ltd. Geotechnical Analyst (Member, Ph. D., Geoenvironment Group, Klohn Crippen Berger Ltd., Vancouver, Canada, park1059@hanmail.net)
2 정회원, 경북대학교 공과대학 토목공학과 (Member, Prof., Dept. of Civil Engrg., Kyungpook National Univ.)
3 계명대학교 토목공학과 부교수 (Associate Prof., Dept. of Civil Engrg., Keimyung Univ.)
* 본 논문에 대한 토의를 원하는 회원은 2006년 10월 31일까지 그 내용을 학회로 보내주시기 바랍니다. 저자의 검토 내용과 함께 논문집에 게재하여 드립니다.

1. Introduction

The concern for soil structures located in active seismic zones is the potential for large displacements in the event of the design earthquake. Such displacements can be very large if soil liquefaction occurs. Remedial measures to reduce liquefaction induced displacements involve densification and/or drainage. Rational assessment of remediation methods requires a reliable prediction of soil response for the design earthquake.

The plastic constitutive model called UBCSAND has been developed for predicting liquefaction response of granular soils (Park et al. 2005). The effective stress UBCSAND procedure is a fully coupled stress-flow plasticity approach in which shear induced contraction and a dilation of the skeleton induce pre- and post-liquefaction response characteristics. The soil skeleton controls the response, and the effect of the pore fluid is purely one of controlling the skeleton volume and bulk stiffness. Most constitutive models are calibrated based on triaxial loading conditions, whereas the UBCSAND model is validated in plane strain condition by capturing a simple shear loading condition similar to earthquake loading. The underlying feature of UBCSAND is simplicity and robustness for practical purposes. This effective stress analysis can estimate the displacements, accelerations and porewater pressure generation and dissipation caused by a specified input motion. Such analyses involve capturing the cyclic simple shear tests with and without static shear stress, and then modeling the soil-structure as a collection of such elements subjected to the design earthquake base motion.

Failure mechanisms due to earthquake loading can be caused not only by a zero effective stress state, generally called liquefaction, but also by large residual deformation with non-zero effective stress. On level ground sites, 100% excess pore pressure rise and liquefaction can occur, but residual displacements are small as there is no "driving" stress. Whereas on sloping ground sites, 100% excess pore pressure rise may not occur, displacement can be very large due to "driving" shear stresses and their pattern of reversal. The 3 categories of shear stress

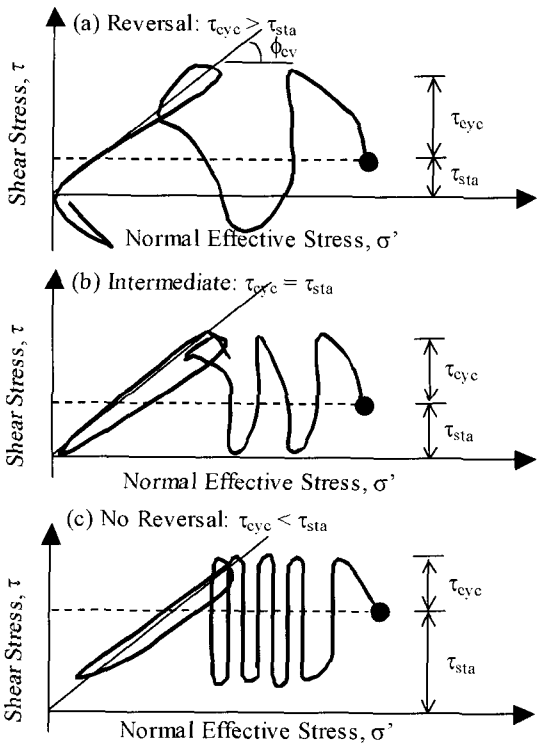

Fig. 1. Patterns of shear stress reversal (Hyodo et al. 1991)

reversal are explained in Figure 1 (Hyodo et al. 1991). The categories depend on whether the cyclic shear stress, τ_{cyc}, is larger, equal to, or smaller than the static shear stress, τ_{sta}.

The effective stress approach including the concept of shear stress reversal can explain the different type of failure pattern that occurs at slope site due to large displacements. In this paper it is applied to capture the cyclic simple shear tests with and without static shear stress. Then, the model is applied to centrifuge test data representing a finite slope and the prediction is compared with the measured response.

2. Effect of Static Shear Stress on Liquefaction

Soil elements beneath dams and slopes and near building structures have an initial static shear stress on horizontal planes. For example, soil elements near the surface of a slope have two characteristics in terms of stress; a driving shear stress, and a low confining stress. In effective stress space, these elements are located near the phase transformation line. Upon earthquake loading the element stress state will move to the phase transfor-

mation line and commence to dilate. This will increase its resistance and lead to limited strain and displacement rather than a failure. The cyclic simple shear tests for these stress conditions showed that the intermediate or no shear stress reversal (one-sided loading) pattern resulted in accumulated large displacements rather than zero effective stress. This one-sided loading pattern was captured in the numerical prediction.

The effect of static shear on liquefaction resistance is briefly reviewed from published laboratory test results. Lee and Seed (1967) found that the larger the initial static shear stress the larger is the liquefaction resistance based on cyclic triaxial compression tests on anisotropically consolidated samples. Since then the effects of initial static shear have been investigated by several researchers using mainly triaxial tests (Vaid and Chern 1983; Ishibashi et al. 1985; Hyodo et al. 1991) and few simple shear tests (Vaid and Finn 1979, Rahhal and Lefebvre 2000). When the cyclic deviator stress is less than the consolidation deviator stress, no shear stress reversal occurs. However, most of the laboratory test data showed shear stress reversal, Figure 1 (a). Vaid and Finn (1979) found that the shear stress reversal pattern could limit the pore pressure generation. They showed conflicting results: either increased or decreased liquefaction resistance due to shear stress reversal. The occurrence of shear stress reversal under a design earthquake seems to be a critical factor and will generate larger displacement irrespective of the stress reversal pattern. In the case of no shear stress reversal, the stress state stays on the failure line, and does not reach zero effective stress, generally called liquefaction, and limits displacements.

From existing data, it is difficult to reach any conclusion about the static shear effect. In section 4, the effect of static shear on air-pluviated loose Fraser River sand data will be discussed.

3. Constitutive Model: UBCSAND

The simplest realistic model for soil is the classic Mohr-Coulomb elastic-plastic model as depicted in Figure 2. Soils are modeled as elastic below the strength envelope and plastic on the strength envelope with plastic shear and volumetric strains increments related by the dilation angle, ψ. This model is really too simple for soils since plastic strains also occur for stress states below the strength envelope. The UBCSAND stress-strain model described herein modifies the Mohr-Coulomb model incorporated in FLAC (Fast Lagrangian Analysis of Continua) Version 4.0 (Itasca 2000) to capture the plastic strains that occur at all stages of loading. Yield loci are assumed to be radial lines of constant stress ratio as shown in Figure 3. Unloading is assumed to be elastic. Reloading induces plastic response but with a stiffened plastic shear modulus.

The plastic shear modulus relates the shear stress and the plastic shear strain and is assumed to be hyperbolic with stress ratio as shown in Figure 4. Moving the yield locus from A to B in Figure 3 requires a plastic shear strain increment, $d\gamma^P$, as shown in Figure 4, and is controlled by the plastic shear modulus, G^P. The associated plastic volumetric strain increment, $d\varepsilon_v^P$, is

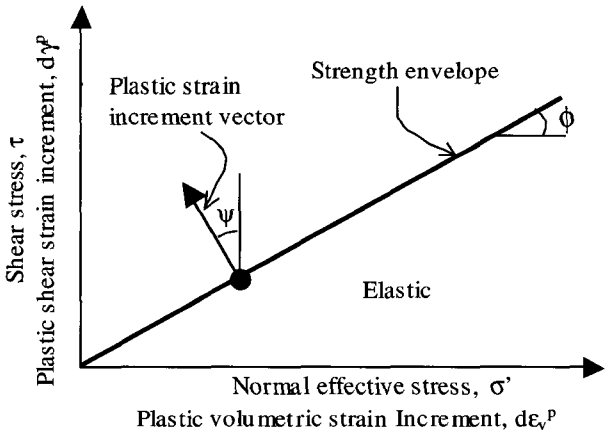

Fig. 2. Classic Mohr-Coulomb model

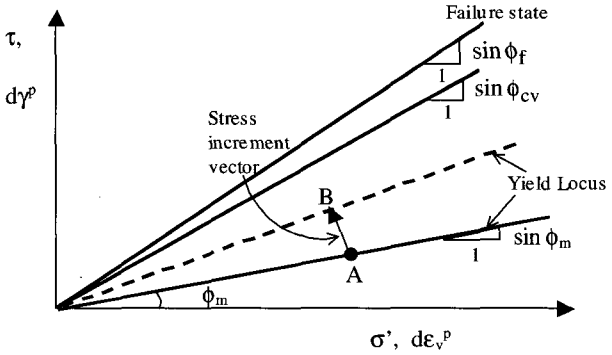

Fig. 3. UBCSAND model

obtained from the mobilized dilation angle ψ_m:

$$d\varepsilon_v^P = d\gamma^P \cdot \sin\psi_m \quad (1)$$

The mobilized dilation angle is based on laboratory data and energy considerations and is approximated by

$$\sin\psi_m = \sin\phi_{cv} - \sin\phi_m \quad (2)$$

where ϕ_{cv} is the phase transformation or constant volume friction angle and ϕ_m describes the current yield locus. A positive value of ψ_m corresponds to contraction. Contraction occurs for stress states below ϕ_{cv} and dilation above as shown in Figure 5.

Additional information on UBCSAND is presented by Park et al. (2005). Elastic and plastic properties for the model are defined as follows.

3.1 Elastic Properties

The elastic bulk modulus, B, and shear modulus, G,

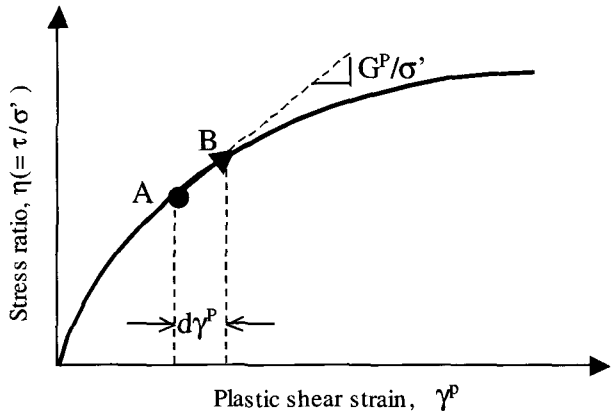

Fig. 4. Hyperbolic stress-strain relationship

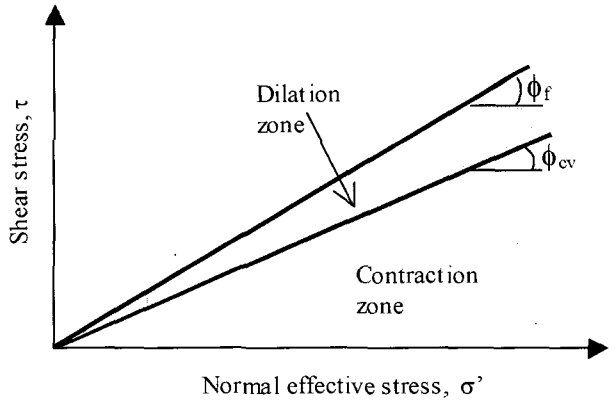

Fig. 5. Zones of shear-induced contraction and dilation

are assumed to be isotropic and stress level dependent. They are described by the following relations:

$$G = k_G^e \cdot P_a \cdot \left(\frac{\sigma'_m}{P_a}\right)^{0.5} \quad (3)$$

$$B = \alpha \cdot G \quad (4)$$

where k_G^e is modulus number, P_a is atmospheric pressure, σ'_m is the mean effective stress in the plane of loading, where $\sigma'_m=(\sigma'_x+\sigma'_y)/2$, $\alpha(=2(1+\nu)/(1-2\nu)/3)$ depends on the Poisson's ratio.

3.2 Plastic Properties

The plastic properties used by the model are the friction angle at failure ϕ_f, the constant volume friction angle ϕ_{cv}, and plastic shear modulus G^P, where

$$G^P = G_i^P \cdot \left(1 - \frac{\eta}{\eta_f} R_f\right)^2 \quad (5)$$

where $G_i^P=k_G^P \cdot P_a \cdot (\sigma'_m/P_a)^{0.4}$ and $k_G^P \approx 8 \cdot (D_r)^4 \cdot k_G^e+100$, η is the current stress ratio $(=\tau/\sigma'_m)$, η_f is the stress ratio at failure, and R_f is the failure ratio used to truncate the hyperbolic relationship.

The position of the yield locus ϕ_m is known for each element at the start of each time step. If the stress ratio increases and plastic strain is predicted, then the yield locus for that element is pushed up by an amount $d\phi_m$ as given by Equation 6. Unloading of stress ratio is considered to be elastic. Upon reloading, the yield locus is set to the stress ratio corresponding to the stress reversal point.

$$d\phi_m = \left(\frac{G^P}{\sigma'_m}\right) \cdot d\gamma^P \quad (6)$$

The response of sand is controlled by the skeleton behavior. A fluid (air water mix) in the pores of the sand acts as a volumetric constraint on the skeleton if drainage is curtailed. It is this constraint that causes the pore pressure rise that can lead to liquefaction. Provided the skeleton or drained behavior is appropriately modeled under monotonic and cyclic loading conditions, and the stiffness of the pore fluid (B_f) and drainage are accounted

for, the liquefaction response can be predicted. This concept is incorporated in UBCSAND.

The elastic and plastic parameters are highly dependent on relative density, which must be considered in any model calibration. These parameters can be selected by calibration to laboratory test data. The response of the model can also be compared to a considerable database for triggering of liquefaction under earthquake loading in the field. This database exists in terms of penetration resistance, typically from cone penetration (CPT) or standard penetration (SPT) tests. A common relationship between $(N_1)_{60}$ values from the SPT and the cyclic stress ratio that triggers liquefaction for a magnitude 7.5 earthquake is given by Youd et al. (2001). Comparing laboratory data based on relative density to field data based on penetration resistance relies upon an approximate conversion, such as that proposed by Skempton (1986):

$$35 < \frac{(N_1)_{60}}{D_r^2} < 55 \qquad (7)$$

Model parameters based on penetration resistance and field observation may be useful for field conditions where it is very difficult to retrieve and test a representative sample. However, this indirect method is not appropriate for simulation of centrifuge models. Calibrations for this case should be based on direct laboratory testing of samples that are prepared in the same manner as the centrifuge model.

4. Calibration with Cyclic Simple Shear Test Data

A series of constant volume simple shear tests was performed on Fraser River sand at the University of British Columbia (UBC) and used as a database to calibrate the numerical model element response. The constant volume test is equivalent to an undrained test and has several advantages: (i) eliminating the error due to compliance, (ii) making the testing easier by eliminating the saturation procedure (Finn and Vaid 1977; Finn et al. 1978). The samples were prepared by air pluviation method, which is normally adopted in centrifuge tests. The sample preparation and testing methods have been described in detail by Sriskandakumar (2004). All samples were placed at D_r = 34% and densified to 40% and 44% under applied pressures of 100 kPa and 200 kPa, respectively. Samples were then subjected to cyclic shear for a range of cyclic stress ratios under constant volume conditions that simulate undrained response.

The tests were carried out without static shear stress first. Four different CSRs (Cyclic Stress Ratio), 0.08, 0.1, 0.12 and 0.15 were used. Typical results of measured response for no static shear are shown in Figure 6. Test data are shown as the heavy lines. The light lines are the numerical predictions and will be discussed later. When CSR = 0.15, it liquefied in one cycle. It was observed that the first and last cycles contributed to large excess pore pressure generation. Once the pore pressure ratio (R_u) reached unity (i.e. vertical effective stress became zero), large strains developed.

Tests were also carried out with static shear stress. The level of initial static shear stress ratio $\alpha(=\tau_{sta}/\sigma_{vo}')$ is defined as driving initial static shear stress, τ_{sta}, to initial vertical effective stress, σ_{vo}' and α = 0.1 is only used. Three different CSRs, 0.06, 0.08 and 0.1 were used for

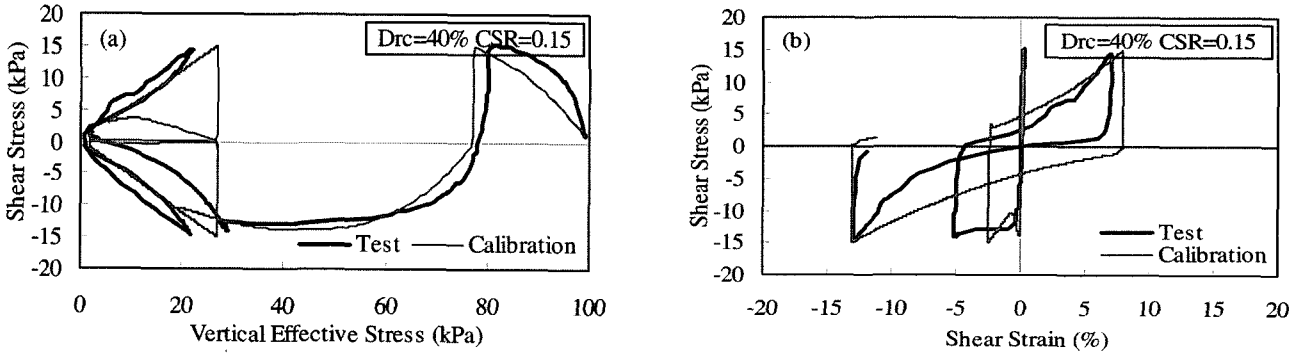

Fig. 6. Measured and predicted (a) stress path and (b) shear stress-strain (α=0.0, CSR=0.15)

both σ'_{vo} = 100 and 200 kPa. The effect of static shear stress reversal is examined by comparing response for different values of τ_{cyc}. Figures 7 and 8 show the results for no reversal, and intermediate reversal patterns, respectively. It may be seen from tests with static shear that once a sample starts to dilate, it follows up and down along the phase transformation line. When no stress reversal occurred, much stiffer behavior is observed. However, the accumulated strains become larger and larger, irrespective of stress reversal patterns. In simple shear tests strains larger than 10% may not be reliable. It is important to capture this behavior in modeling liquefaction response of slopes.

The CSR versus number of cycles to liquefaction is shown both with and without static shear stress in Figure 9. The liquefaction was defined as $\gamma > 3.75\%$. At this point, i.e. $\gamma \sim 3.75\%$, R_u is nearly 90 - 95%. The important conclusion is that, without static shear stress ($\alpha = 0$), the increase in D_r caused by increasing the stress from 100 kPa to 200 kPa seems to more than offset the expected reduction due to the confining stress effect (K_σ effect) as shown in Figure 9. On the other hand, with static shear stress the difference in liquefaction resistance caused by stress densification effect is no longer pronounced as shown in Figure 9 (α = 0.1). In summary, the initial static shear stress on loose Fraser River sand under applied pressure of 100 kPa leads to much less reduction on liquefaction resistance compared to 200 kPa. This finding can infer that at very small confining stress the initial static shear stress gives more resistance to liquefaction due to more dilating behavior of sand. This is consistent with Rahhal and Lefebvre (2000)'s finding based on direct simple shear tests.

The calibration was carried out in the same way as the tests, i.e. under constant volume. The single element was used. The elastic and plastic parameters selected for calibration were the same for all cases having the same relative density after consolidation (D_{rc}) and listed in Table 1 (Park and Kim 2006). The predicted stress-strain and stress paths are shown in Figures 6-8 as "light" lines. The predictions give a reasonable representation of the observed response, although the cyclic mobility was not captured as shown in Figure 7 (b). The predicted triggering of liquefaction with and without static shear stress is

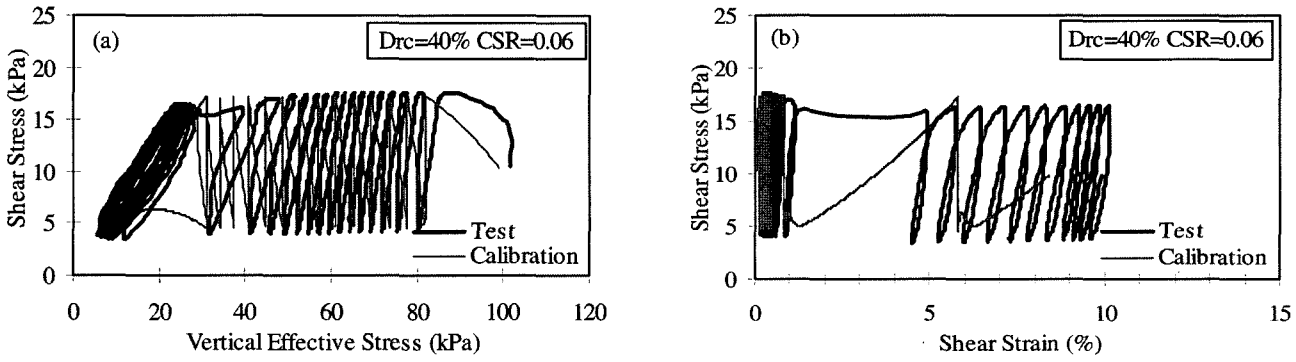

Fig. 7. Measured and predicted (a) stress path and (b) shear stress-strain (α=0.1, CSR=0.06)

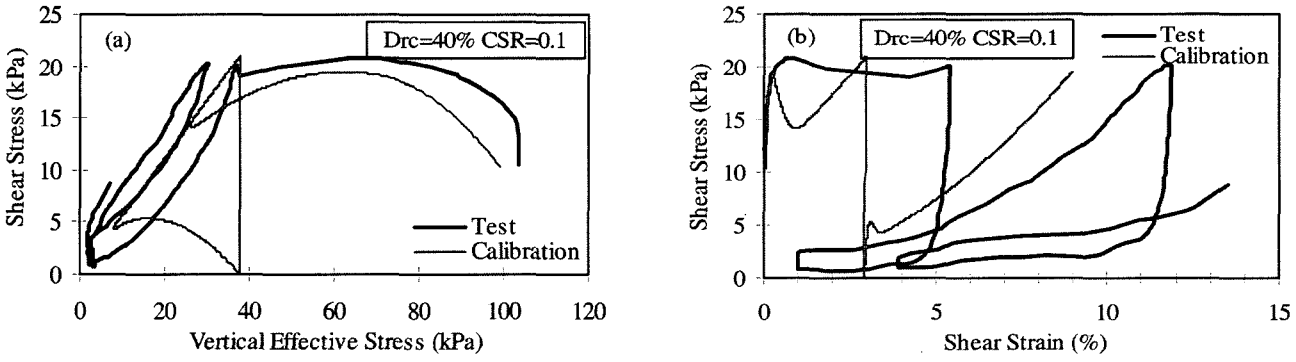

Fig. 8. Measured and predicted (a) stress path and (b) shear stress-strain (α=0.1, CSR=0.1)

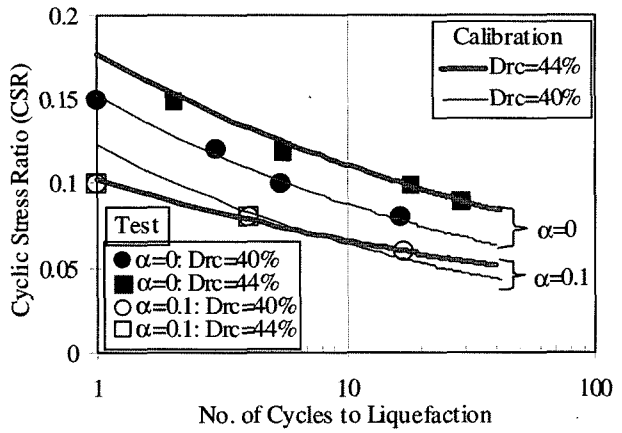

Fig. 9. Predicted and measured liquefaction response of Fraser River sand with and without static shear stress

shown as the lines in Figure 9. The predicted and measured liquefaction responses are in close agreement.

5. Numerical Prediction of a Centrifuge Test

A series of dynamic centrifuge tests has been completed at the Centre for Cold Ocean Research (C-CORE) for the cooperative research project between UBC, C-CORE, Memorial University of Newfoundland and industrial partners. Detailed information regarding these tests is available on the web site (http://www.civil.ubc.ca/liquefaction). A numerical prediction using UBCSAND was made of one centrifuge model test. In the centrifuge test, a small model is subjected to a high acceleration field during the test. This has the effect of increasing its stresses by the ratio of the induced acceleration divided by the acceleration of gravity. This ratio is 70 for this centrifuge test. The centrifuge model under the increased acceleration field can also be thought of as representing a prototype that is 70 times larger than the actual small-scaled model. Results from the centrifuge test can be presented at either the model or prototype scale. The prototype scale is used for this paper.

While in flight, a motion simulating an earthquake time history is applied to the base of the model. For dynamic similitude at the model scale, the earthquake time scale must be decreased by a factor of 70, and the earthquake acceleration increased by the same factor. The engineering coefficient of permeability k will also be increased by this same factor due to the increased unit weight of the fluid. k should be decreased for hydraulic similitude, although it is not necessary to model a specific k. It is common to use a fluid in the test that is 30 to 60 times more viscous than water to prevent rapid rates of dissipation that might unduly curtail liquefaction effects. In this centrifuge test, a fluid 35 times more viscous than water was used.

Fraser River sand was used for this centrifuge test and its liquefaction and permeability (at 1 g using water as pore fluid) properties were obtained from laboratory tests including simple shear tests (http://www.civil.ubc.ca/liquefaction). The measured liquefaction resistance together with the UBCSAND prediction for Fraser River sand is shown in Figure 9.

5.1 Finite Steep Slope Model

The cross section and instrumentation for centrifuge model is shown in Figure 10 and comprises a steep 2:1 slope in loose Fraser River sand with D_r = 40%. The selected earthquake record was baseline corrected and then applied to the centrifuge test. The input motions for centrifuge test and numerical modeling are the same as shown in Figure 11. The container for centrifuge model was rigid and this was simulated in the FLAC model by applying the same input motion to the vertical sides as well as the base. The key inputs for the centrifuge model are listed in Table 1 (Park and Kim 2006). Pore pressures and accelerations were measured away from the face of the slope, approximating free field conditions, as well as adjacent to the slope.

The predicted and observed accelerations and excess pore pressures in the free field are shown in Figures 12 and 13. The dotted line in Figure 13 indicates the initial vertical effective stress calculated from the planned coordinates. This line may not be directly applicable to measured excess pore pressures since actual locations of

Table 1. Input parameters for Fraser River sand

k_G^e	α	k_G^p	ϕ_{cv}	ϕ_f	R_f
867	0.75	282	33°	34°	0.92

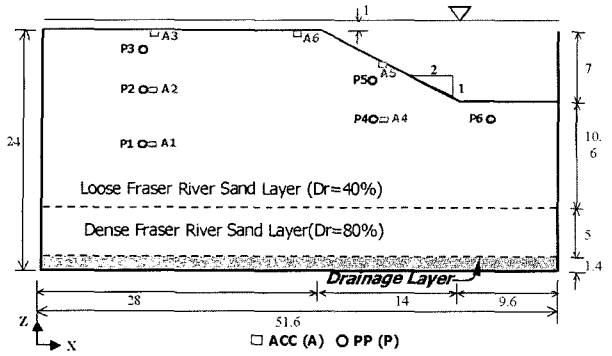

Fig. 10. Cross section and instrumentation of centrifuge model (unit: m in prototype)

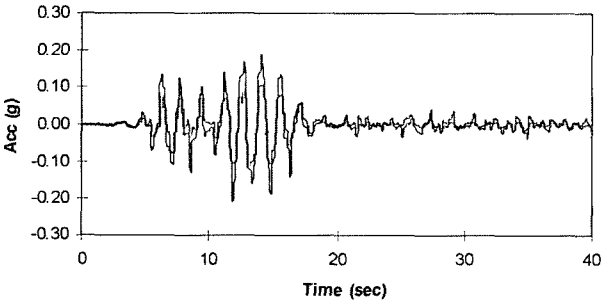

Fig. 11. Earthquake input motion

some transducers are not exactly the same as planned locations (C-CORE, 2004). As expected, R_u of 100% (i.e., liquefaction) at shallow depth and reduced accelerations are seen as similar trends observed in the level ground liquefaction centrifuge test (Byrne et al. 2004).

The accelerations and excess pore pressures near the slope are shown in Figures 14 and 15. It may be seen in Figure 14 that there is little or no reduction in the accelerations. Instead, large upslope acceleration spikes occur. Excess pore pressures are shown in Figure 15. Large negative excess pore pressure spikes occur, which coincide in time with the upslope acceleration spikes. The slope is steep and the upslope acceleration of the base tends to induce failure of the slope and relative downslope movement. The soil dilates as it shears in the downslope direction, producing negative pore pressures which stiffen the shear modulus. Enough strength is mobilized through this dilation to arrest the downslope movement and gives rise to the acceleration spike.

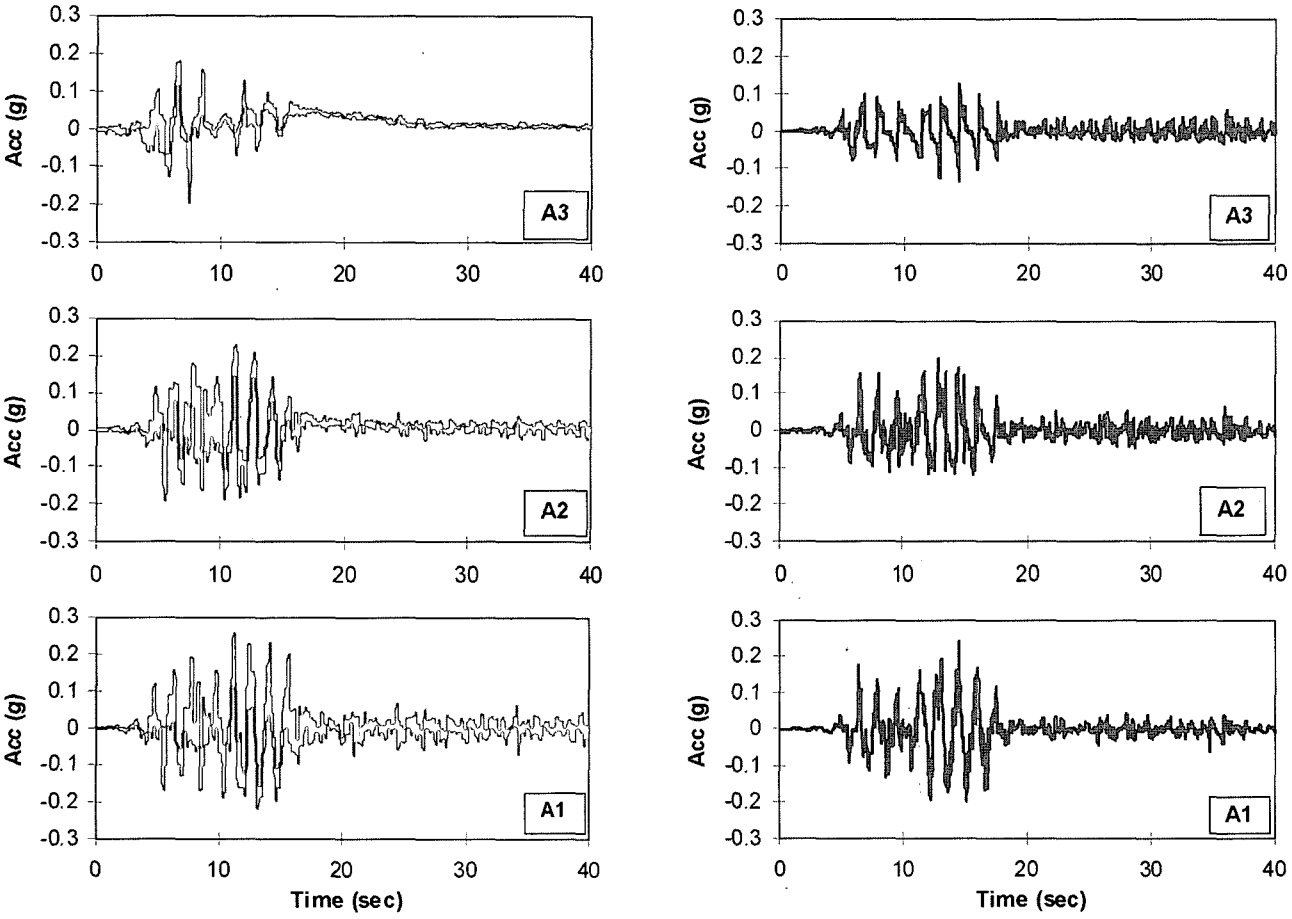

Fig. 12. Measured (left) and predicted (right) accelerations (Acc) in the free field

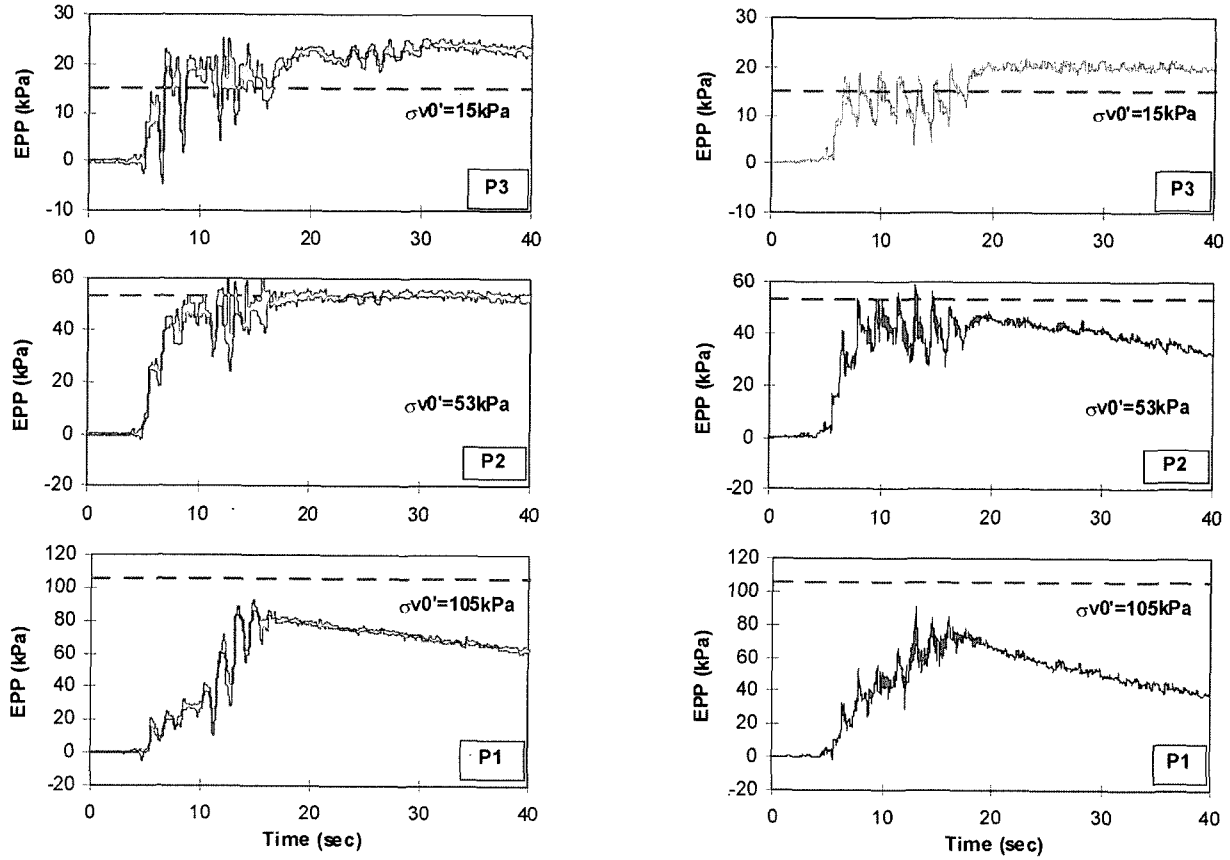

Fig. 13. Measured (left) and predicted (right) excess pore pressures (EPP) in the free field

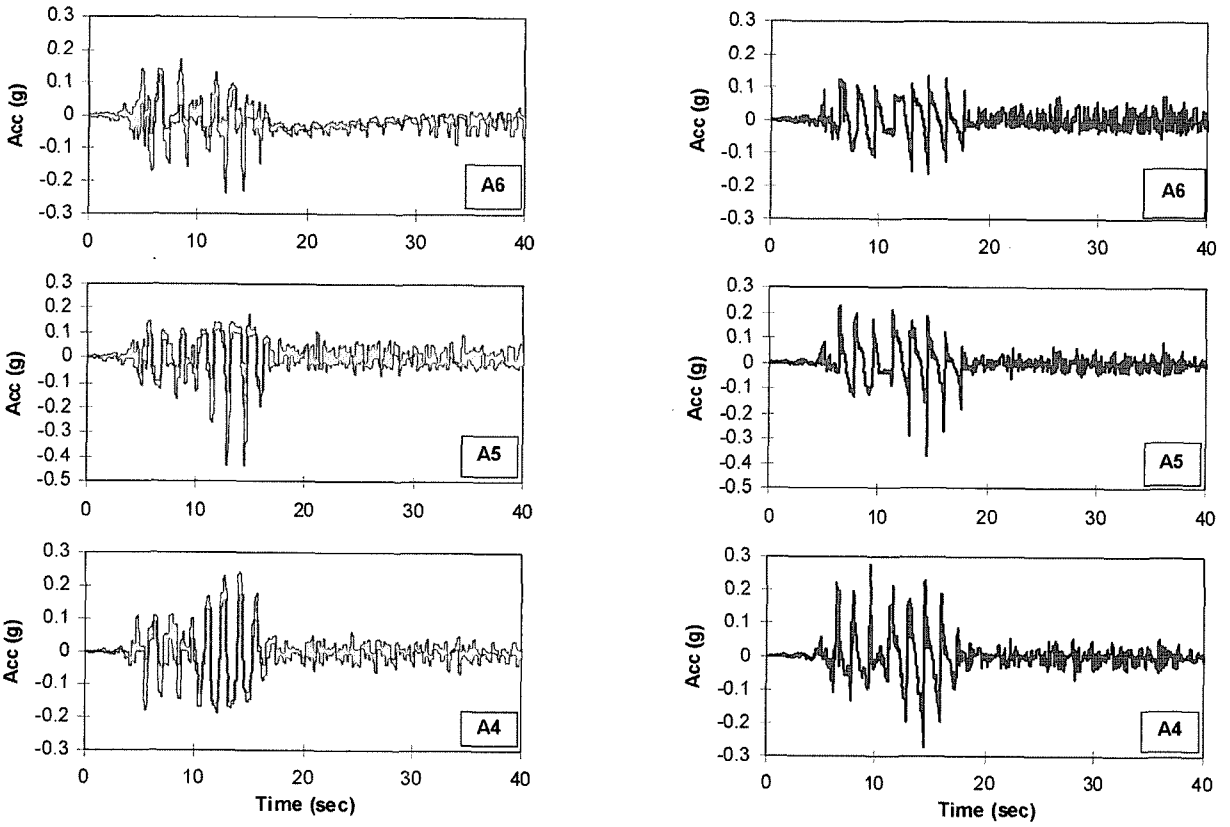

Fig. 14. Measured (left) and predicted (right) accelerations (Acc) near the slope

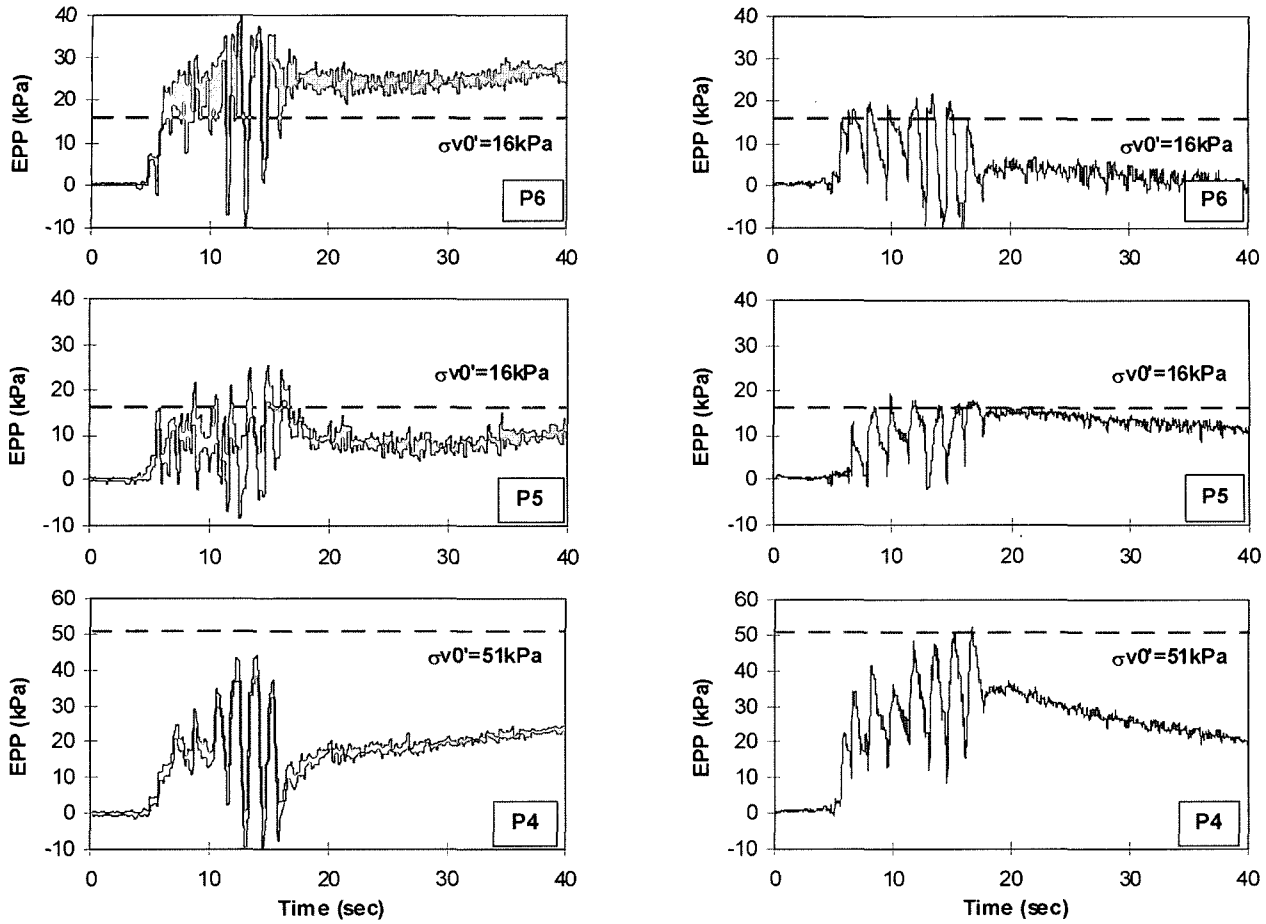

Fig. 15. Measured (left) and predicted (right) excess pore pressures (EPP) near the slope

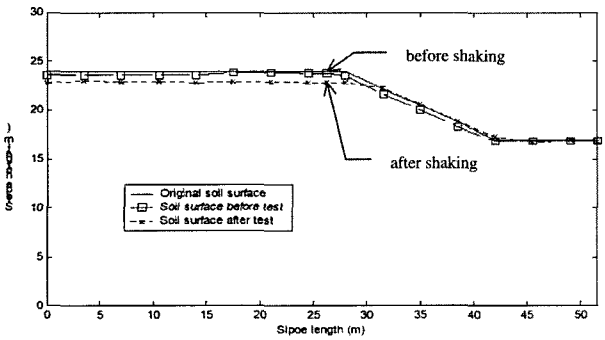

Fig. 16. Measured displacements from centrifuge test (after C-CORE 2004)

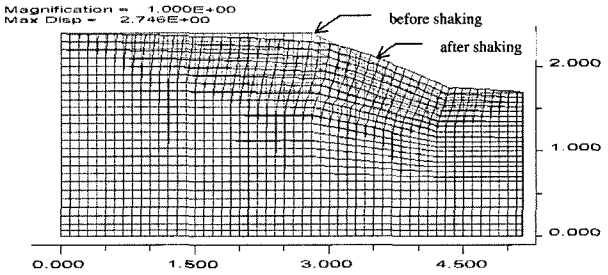

Fig. 17. Predicted displacements for centrifuge model using UBCSAND (axis scale = x 10)

UBCSAND provides a reasonable prediction of the accelerations and pore pressure response for the free field. More differences are observed for locations near the slope. Some of these differences are due to UBCSAND under predicting the dilative spikes. The measured and predicted displacements after shaking are shown in Figures 16 and 17. The predicted maximum displacement is about 2.7 m. It may be seen that both the magnitude and pattern of displacements are in general agreement.

In summary,

(a) UBCSAND provides reasonable agreement with this centrifuge test, although further study is needed for locations close to the sloping face,

(b) a decrease in accelerations after liquefaction was observed in the free field back from the slope face,

(c) large upslope acceleration spikes occurred near the slope,

(d) a decrease in pore pressure due to dilation corresponded with these upslope acceleration spikes, and
(e) the dilative spikes prevented very large displacements from occurring in this homogeneous fine sand model.

6. Summary

A fully coupled effective stress dynamic analysis procedure has been presented. The procedure is first calibrated by comparison with laboratory element test data and then validated by comparison with a centrifuge model test.

Element tests show that initial small density increase can overcome the K_σ effect. The effect of initial static shear stress on liquefaction resistance depends on the level of applied confining stress.

Centrifuge model representing a slope condition in homogeneous loose Fraser River sand was examined and numerically modeled. The results showed that large upslope acceleration spikes occurred near the face of the slope after liquefaction. These acceleration spikes corresponded with large negative excess pore pressure spikes associated with dilation. It is the increase in effective stress associated with these negative pore pressure spikes that curtails the displacements and makes the slope more stable than might be expected under cyclic loading. The overall pattern of predicted response is in reasonable agreement with the measurements.

Acknowledgement

The first author is grateful for the financial support provided by Dr. P.M. Byrne at the University of British Columbia and the National Sciences and Engineering Research Council (NSERC) of Canada.

References

1. 박성식, 김영수, Byrne, P.M., 김대만 (2005), "액상화해석을 위한 간단한 구성모델", 한국 지반공학회 논문집, 제21권, 제8호, pp.27-35.
2. 박성식, 김영수 (2006), "유효응력모델을 이용한 동적 원심모형실험의 수치해석", 한국 지반공학회 논문집, 제22권, 제1호, pp.25-34.
3. Byrne, P.M., Park, S.-S., Beaty, M., Sharp, M., Gonzalez, L. and Abdoun, T. (2004), Numerical modeling of liquefaction and comparison with centrifuge tests. *Canadian Geotechnical Journal*, 41(2), 193-211.
4. C-CORE (2004), Earthquake induced damage mitigation from soil liquefaction. Data report- centrifuge tests CT2. Contract report prepared for the University of British Columbia, C-CORE Report R-04-027-145, July 2004.
5. Finn, W.D.L. and Vaid, Y.P. (1977), Liquefaction potential from drained constant volume cyclic simple shear tests. In Proceedings of the Sixth World Conference on Earthquake Engineering, Vol.3, pp.2157-2162.
6. Finn, W.D.L., Vaid, Y.P., and Bhatia, S.K. (1978), Constant volume cyclic simple shear testing. In Proceedings of the Second International Conference on Microzonation for safer construction- research and application, Vol.2, pp.839-851.
7. Hyodo, M., Murata, H., Yasufuku, N. and Fujii, T. (1991), Undrained cyclic shear strength and residual shear strain of saturated sand by cyclic triaxial tests, Soils and Foundations, 31 (3): 60-76.
8. Ishibashi, I., Kawamura, M. and Bhatia, S.K. (1985), Effects of initial shear on cyclic behavior of sand, Journal of Geotechnical Engineering, 111 (12): 1395-1410.
9. Itasca (2000), FLAC, version 4.0. Itasca Consulting Group Inc., Minneapolis.
10. Lee, K.L. and Seed, H.B. (1967), Drained strength characteristics of sands. *Journal of the Soil Mechanics and Foundations Division*, 93 (SM6): 117-141.
11. Rahhal, M.E. and Lefebvre, G. (2000), Understanding the effect of a static driving shear stress on the liquefaction resistance of medium dense granular soils, Soil Dynamics and Earthquake Engineering, 20: 397-404.
12. Skempton, A.W. (1986), Standard penetration test procedures and the effects in sands of overburden pressure, relative density, particle size, ageing and overconsolidation, Geotechnique 36, No. 3: 425-447.
13. Sriskandakumar, S. (2004), Cyclic loading response of Fraser River sand for validation of numerical models simulating centrifuge tests. M.A.Sc. Thesis, Department of Civil Engineering, University of British Columbia, Canada.
14. Vaid, Y.P. and Chern, J.C. (1983), Effect of static shear on resistance to liquefaction. Soils and Foundations, 23 (1): 47-60.
15. Vaid, Y.P. and Finn, W.D.L. (1979), Static shear and liquefaction potential, *Journal of Geotechnical Engineering*, 105 (10): 1233-1246.
16. Youd, T.L., Idriss, I.M., Andrus, R.D., Arango, I., Castro, G., Christian, J.T., Dobry, R., Finn, W.D.L., Harder Jr., L.F., Hynes, M.E., Ishihara, K., Koester, J.P., Liao, S., Marcuson III, W.F., Martin, G.R., Mitchell, J.K., Moriwaki, Y., Power, M.S., Robertson, P.K., Seed, R.B. and Stokoe, K.H. (2001), Liquefaction Resistance of Soils: Summary Report from the 1996 NCEER and 1998 NCEER/NSF Workshops on Evaluation of Liquefaction Resistance of Soils. *Journal of Geotechnical and Geoenvironmental Engineering*, 127(10): 817-833.

(received on Dec. 29, 2005, accepted on Apr. 17, 2006)